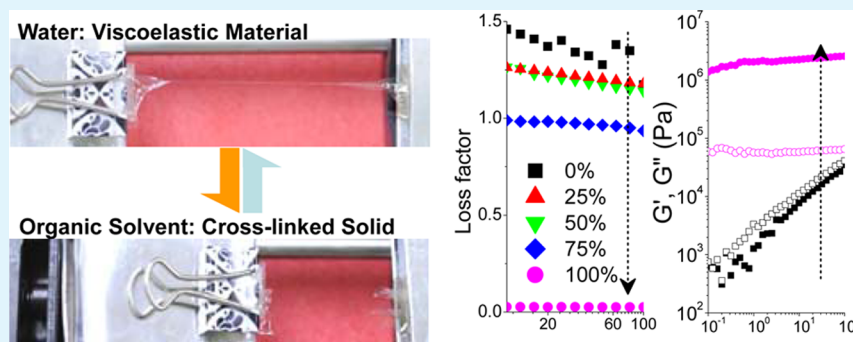


Large-Scale Solvent Driven Actuation of Polyelectrolyte Multilayers Based on Modulation of Dynamic Secondary Interactions

Yuanqing Gu,[†] Xiayun Huang,[‡] Clinton G. Wiener,[†] Bryan D. Vogt,[†] and Nicole S. Zacharia*,[†][†]Department of Polymer Engineering, University of Akron, Akron, Ohio 44325, United States[‡]Department of Mechanical Engineering, Texas A&M University, College Station, Texas 77843, United States**S** Supporting Information

ABSTRACT: Polyelectrolyte multilayers (PEMs), assembled from weak polyelectrolytes, have often been proposed for use as smart or responsive materials. However, such response to chemical stimuli has been limited to aqueous environments with variations in ionic strength or pH. In this work, a large in magnitude and reversible transition in both the swelling/shrinking and the viscoelastic behavior of branched polyethylenimine/poly(acrylic acid) multilayers was realized in response to exposure with various polar organic solvents (e.g., ethanol, dimethyl sulfoxide, and tetrahydrofuran). The swelling of the PEM decreases with an addition of organic content in the organic solvent/water mixture, and the film contracts without dissolution in pure organic solvent. This large response is due to both the change in dielectric constant of the medium surrounding the film as well as an increase in hydrophobic interactions within the film. The deswelling and shrinking behavior in organic solvent significantly enhances its elasticity, resulting in a stepwise transition from an initially liquid-like film swollen in pure water to a rigid solid in pure organic solvents. This unique and recoverable transition in the swelling/shrinking behaviors and the rheological performances of weak polyelectrolyte multilayer film in organic solvents is much larger than changes due to ionic strength or pH, and it enables large scale actuation of a freestanding PEM. The current study opens a critical pathway toward the development of smart artificial materials.

KEYWORDS: polyelectrolyte, layer-by-layer assembly, thin films, organic liquids, actuations

1. INTRODUCTION

Polyelectrolyte multilayers (PEMs) have been examined for possible use in a wide range of applications, such as sensors, actuators or other responsive materials, self-cleaning surfaces, anticorrosion coatings, barrier materials, and separation membranes.^{1,2} The characteristic property of these thin films is that they are assembled through secondary interactions, but this has also in some sense been a limitation for them as well. Response is often based on weakening the strength of electrostatic interactions between hydrated ion pairs, swelling the films and making them softer. For barrier materials or applications where diffusion through the multilayer is important, the free volume in these materials is predetermined by a combination of the strength of interactions between the polyelectrolytes and the solution chain conformations.³ Presented here is a simple and general way to overcome these limitations by changing the dielectric constant and hydrophobicity of the medium surrounding the polyelectrolyte

assembly, potentially enabling a great deal of new functionality in these materials. Changing free volume on demand in a polymer thin film could potentially be important for certain properties.

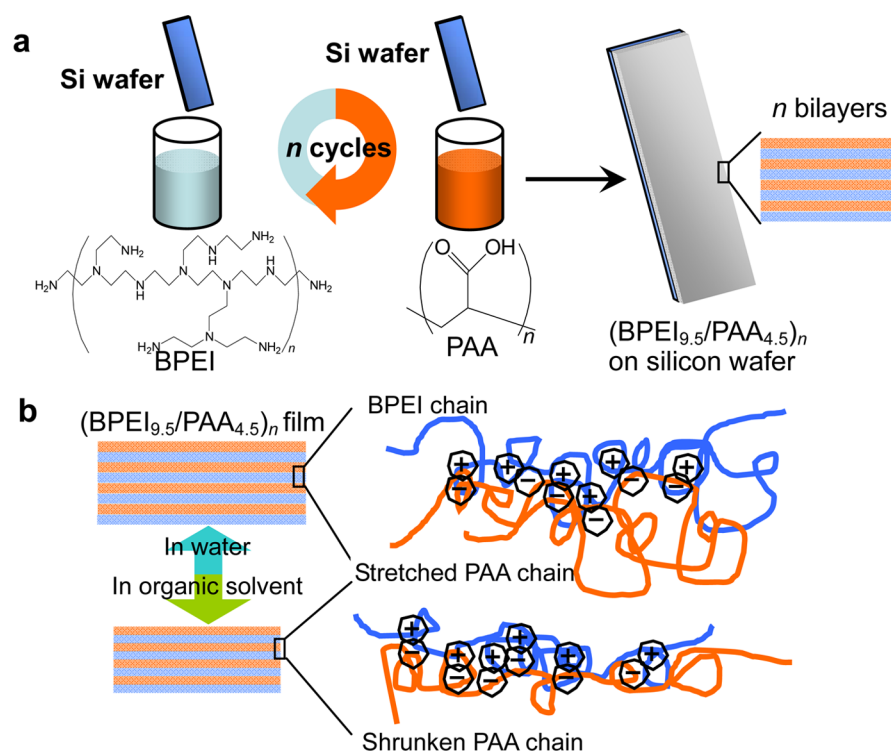
PEMs are made by directing the self-assembly of polyelectrolytes (PEs) onto a surface, using a method called layer-by-layer (LbL), usually through a series of sequential dipping steps. This entropy-driven process^{4,5} is a facile method for assembling multivalent macromolecules as well as other types of materials (colloids, biological materials, some multivalent small molecules) using electrostatics, van der Waals interactions, hydrogen bonds, or even covalent bonds, and the LbL technique gives films with great control over nanoscale placement of film components.² In addition to two-dimensional flat surfaces, various substrates

Received: October 31, 2014

Accepted: December 24, 2014

Published: December 24, 2014

Scheme 1. Schematic Depiction of the LbL Assembly Process (a) As Well As a Schematic Depiction of the Film Densification Process upon Exposure to Organic Solvent (b)



ranging from nanoparticles, nanowires, micelles,⁶ proteins,⁷ and three-dimensionally structured substances such as porous anodic alumina membranes,⁸ random hierarchically structured networks,^{9,10} and even biological materials such as butterfly wings can be coated by LbL technique.¹¹

Responsiveness in PEMs is usually based on achieving a modulation in the charge–charge interactions within the films. For strong PEs, this usually means changing ionic strength of a surrounding aqueous medium, whereas for weak PEs charge density can also be modulated by ionic strength as well as pH or even other external stimuli, such as electric fields.¹² The charge density of certain weak PEs with particularly labile functional groups, such as carboxylic acids, can be easily influenced by the nearby presence of other charged molecules (such as other PEs), especially in the solid state.¹³ Varying charge–charge interactions will then affect chain conformation, solubility, and ability of the PEs to act as hydrogen bonding donors or acceptors. The dynamic nature of the interactions holding together the PE chains leads to certain unique properties. For example, polyethylenimine/poly(acrylic acid) multilayer based electrodes are able to self-heal upon exposure to water;¹⁴ the swelling of hydrophilic PEM films can be controlled by changing the ionization ratio and charge density of the PEs in the PEMs to regulate the internal ionic cross-links.¹² This reversible stimuli-responsive performance of weak PE containing PEMs holds a great promise for application in drug delivery, separation, and smart sensors.¹⁵ However, achieving response in PEMs through a chemical stimulus has thus far been limited to exposing these films to various types of aqueous solutions, either changing the charge density within the film or softening the ionic bond pairs.

Organic solvents, however, are known to have significant effects on the physicochemical properties of PEs.¹⁶ The low dielectric constant of organic solvents inhibits the ionization of PEs, and the low polarity of the environment induces changes in

the chain conformation of the PEs and increases the internal hydrophobic interactions between polymer backbones.¹⁷ This phenomena of aggregation of PE chains are universal to most organic solvents. Although this strong change in PE solution behaviors in response to exposure to organic solvents is known, it has not thus far been widely used to achieve response or changes in properties in PEMs. There are several reports of LbL assembly using organic solvents,^{18–20} and in one of these, the addition of tetrahydrofuran to a dendrimer solution resulted in a mechanically stiffer capsule. In contrast, several reports show exposure of PEM capsules to water/alcohol or water/acetone solutions actually softens and increases the permeability of these capsules.^{21–23} Also, PEMs have been employed as membranes for water/alcohol separations based on differences in diffusion and solubility of those solvents in the PEM films.²⁴

In this work, a reversible, large scale swelling/shrinking response accompanied by changes in viscoelastic properties is achieved with electrostatics mediated PEM assemblies fabricated with branched polyethylenimine (BPEI) and poly(acrylic acid) (PAA) by taking advantage of changes in secondary interactions upon exposure to polar organic solvents (e.g., ethanol, dimethyl sulfoxide, and tetrahydrofuran). The BPEI/PAA film contracts in the presence of organic solvent, in contrast to the swelling seen in water. The interactions in question, electrostatic ion pairs as well as hydrophobic interactions, are dynamic, and therefore, this response is a reversible one that can be repeated many times. After densification in pure organic solvent, the film thickness will either recover to its original value by interaction with ambient humidity or the densified thickness can be permanently fixed through facile thermal amide cross-linking between BPEI and PAA. The swollen film in pure water behaves as a viscous liquid that gradually changes to an elastic solid by the addition of organic liquid to the water. In pure organic solvent, the film behaves as a rigid cross-linked material due to the enhanced

internal interactions and reduced film thickness. Large scale, reversible actuation of a free-standing PEM is demonstrated based on this behavior, showing potential for applications in sensing, smart switches, valves, and motors.

2. EXPERIMENTAL SECTION

2.1. Materials. Branched polyethylenimine (BPEI, $M_w = 25\,000$, catalog No. 408727), poly(diallyldimethylammonium chloride) (PDAC, average $M_w = 100\,000$ – $200\,000$, 20 wt % in H_2O , catalog No. 409014), poly(sodium 4-styrenesulfonate) (SPS, average $M_w \sim 70\,000$, catalog No. 243051), ethanol (catalog No. E7023), dimethyl sulfoxide (DMSO, catalog No. D4540), tetrahydrofuran (THF, catalog No. 360589), sodium chloride (catalog No. S9888), sodium hydroxide (catalog No. 221465), hydrochloric acid (catalog No. 320331), sulfuric acid (catalog No. 320501), and hydrogen peroxide (catalog No. 216763) were purchased from Sigma-Aldrich. Polyacrylic acid (PAA, $M_w = 50\,000$, 25 wt % solution, catalog No. 00627) was purchased from Polysciences. Deionized (DI) water used in all experiments from a Milli-Q-DQ-3 system (Millipore, Bedford, MA, U.S.A.) with resistivity of 18.2 M Ω . All materials were used as received without further purification.

Piranha solution was prepared by mixing 98% sulfuric acid with 30% hydrogen peroxide with a volume ratio of $v/v = 7/3$. BPEI solution was prepared at 80 mM with respect to the amine group of BPEI in DI water. The solution was stirred overnight and the pH was adjusted to 9.5 by adding 0.1 M hydrochloride solution. Similarly, PAA solution was prepared at 60 mM with respect to the carboxyl group of PAA in DI water and was stirred overnight; subsequently, the pH was adjusted to 4.5 by adding 0.1 M sodium hydroxide solution. All PE solutions were filtered prior to use.

2.2. Film Assembly. PEMs were LbL assembled through electrostatic interactions on silicon wafers as shown in Scheme 1a.²⁵ Polished silicon wafer was employed here as the substrate because it is nearly atomically flat and the high refractive index of silicon provides a good contrast to PEMs for high resolution spectra. Silicon wafers were first cleaned by immersion in a freshly prepared piranha solution at room temperature for 4 h, rinsed with excess DI water until neutral, dried by nitrogen flow, and then plasma treated for 5 min prior to use. The assembly of PEMs proceeded sequentially at room temperature using a StratoSequence VI dipper (NanoStrata Inc., U.S.A.). Briefly, the dry silicon wafers were first exposed to the BPEI solution for 10 min and then washed by three separate DI water rinse baths of 1 min each. Subsequently, these substrates were exposed to the PAA solution for 10 min and washed with DI water in an identical manner. Thus, a thin BPEI/PAA bilayer was assembled on the silicon wafer surface. By repeating the BPEI/PAA deposition cycle n times, the desired number of BPEI/PAA bilayers (denoted as $(BPEI_{9.5}/PAA_{4.5})_n$ hereafter) were deposited on the silicon wafer. These PEM films were dried at room temperature ($\sim 25\text{ }^\circ\text{C}$) and atmospheric relative humidity (RH $\sim 70\%$) for 24 h prior to characterizations. To prepare the PEM sample for rheological characterization, the $(BPEI_{9.5}/PAA_{4.5})_{50}$ film was LbL assembled on a cleaned polystyrene substrate following the above procedure. After drying, the film was peeled off of the polystyrene substrate and cut into a circle with a diameter of 8.0 mm. $(PDAC/SPS)_{30}$ films were fabricated through the same process by using PDAC aqueous solution (20 mM with respect to amine group) and SPS aqueous solution (20 mM with respect to sulfonate group) or PDAC in 0.1 M sodium chloride aqueous solution (20 mM with respect to amine group) and SPS in 0.1 M sodium chloride aqueous solution (20 mM with respect to sulfonate group).

For thermal cross-linking treatment of the PEM film, solvent exposed $(BPEI_{9.5}/PAA_{4.5})_n$ films were heated at $180\text{ }^\circ\text{C}$ for 2 h and then cooled to ambient temperature as described previously.²⁵

The actuating film was prepared by successive LbL assembly of 50 $BPEI_{9.5}/PAA_{4.5}$ bilayers and 50 $PDAC/SPS$ bilayers on a cleaned polystyrene substrate following the same LbL procedures. Due to the weak interaction between PEMs and hydrophobic polystyrene substrate, the as-deposited $(BPEI_{9.5}/PAA_{4.5})_{50}/(PDAC/SPS)_{50}$ film can be peeled off of the substrate, resulting in a free-standing PEM film.

2.3. Characterization. The dry film thickness of the as-prepared $(BPEI_{9.5}/PAA_{4.5})_n$ films was determined by the average value from five different positions of the film using a stylus profilometer ($P\bar{6}$, KLA Tencor Instruments, Milpitas, CA, U.S.A.). Fourier transform infrared (FT-IR) spectra were acquired by an FT-IR spectrometer (Alpha-P, Bruker Optics, Billerica, MA, U.S.A.) with transmission mode. The samples were tested immediately after vacuum drying overnight, and all measurements were done at room temperature ($\sim 25\text{ }^\circ\text{C}$) with the atmospheric RH of $\sim 70\%$. Dynamic light scattering (DLS) analyses were performed using a zeta potential analyzer (ZetaPALS, Brookhaven Instruments, Holtsville, NY, U.S.A.).

A variable angle spectroscopic ellipsometer (VASE, M-2000 UV-visible–NIR [240–1700 nm] J. A. Woollam Co., Inc., Lincoln, NE, U.S.A.) equipped with a temperature controlled liquid cell was employed for in situ characterization of the PEM films to determine their thickness and optical constants in both dry and swollen states (Scheme S1, see Supporting Information). The cell geometry dictated the angle of incidence to be 75° . Due to absorption in the ultraviolet and near-infrared light region by the solvents, a limited wavelength range from 300 to 1150 nm was used for the recursive fits. Standard window correction protocols using a silicon wafer with thermal oxide (25.0 nm) as the reference were utilized prior to each measurement.²⁶ To fit the ellipsometry data, a four-layer model consisting of a silicon substrate layer (Si Temp JAW, Temp Library, temperature $25\text{ }^\circ\text{C}$), a fixed Si-SiO₂ interface layer (INTR JAW, thickness 1.0 nm), a thermal oxide layer (SiO₂ JAW, thickness 0.8 nm), and a Cauchy layer (with thickness, A and B free fit parameters) for the PEM was employed in Complete EASE (J. A. Woollam, Co., Inc., Lincoln, NE, U.S.A.).²⁷ All in situ measurements were performed at a fixed temperature of $25\text{ }^\circ\text{C}$. The PEM film was initially measured in the dry state. After 1 min, the solvent of interest was carefully charged to the cell using a syringe to exclude bubbles. For modeling of the ellipsometric data, the fixed refractive index for the corresponding solution was applied. These optical properties of the solution were established by the corresponding control solution on silicon wafers, and the determined refractive indices at 632 nm for water, ethanol, DMSO, and THF are 1.333, 1.478, 1.361, 1.405, respectively. The PEM sample was equilibrated in each solution for 15 min.

The reversible thickness change of $(BPEI_{9.5}/PAA_{4.5})_6$ film in DI water and pure ethanol was monitored by in situ ellipsometry at $25\text{ }^\circ\text{C}$ as described above. The $(BPEI_{9.5}/PAA_{4.5})_6$ film was loaded in the liquid cell and first allowed to swell in DI water for 15 min to determine the equilibrium swelling. The DI water directly from the purification system has a pH of 6.6, slightly lower than neutral due to carbon dioxide, which is not removed by the purification system. After vacuum drying for 3 h, the film was soaked in pure ethanol by an identical process. This successive swelling/shrinking cycle in DI water and pure ethanol was repeated 10 times at room temperature.

For recovery of THF treated $(BPEI_{9.5}/PAA_{4.5})_6$ film in the ambient environment, the $(BPEI_{9.5}/PAA_{4.5})_6$ film was immersed in pure THF for 30 min and then vacuum-dried overnight. The film was then immediately subjected to in situ ellipsometry measurement in air ($25\text{ }^\circ\text{C}$, RH $\sim 70\%$).

To acquire information about both thickness and mass of the films, a $(BPEI_{9.5}/PAA_{4.5})_6$ film was deposited on Q-Sense silica-coated quartz crystal sensor (QX 335) and the response to solvent was probed by a Q-Sense E1 QCM-D instrument (Q-Sense, Gothenburg, Sweden) using the ellipsometry QCM-D cell (QELM 401) to enable simultaneous measurement of thickness by spectroscopic ellipsometry. The crystal was cleaned with DI water and vacuum-dried overnight prior to the film coating procedure to avoid contamination. PAA and BPEI were alternatively LbL assembled through the above-mentioned process, and then rinsed with DI water and vacuum-dried overnight. Thereafter, the as-prepared $(BPEI_{9.5}/PAA_{4.5})_6$ film on the quartz crystal was loaded in the QCM-D flow chamber. A stable baseline of QCM-D was first obtained to determine the dry film, and then DI water was pumped across the film at a flow rate of $150\text{ }\mu\text{L}/\text{min}$ until the thickness reached apparent equilibrium. Subsequently, the ethanol content was increased stepwise after reaching equilibrium until pure ethanol was applied (10 vol % per step), and then decreased stepwise to DI water. QCM-D data

were processed with QTools (Q-Sense) to obtain the mass change of the film as a function of the solution concentration. The raw data were corrected by the frequency and dissipation from the bare silica sensor with the same ethanol–water mixtures to remove effects associated with viscosity differences of the solutions. The mass of liquid in film was calculated by subtracting the initial dry film mass from the total mass.

Oscillatory shear measurements were performed on a strain-controlled Advanced Rheometric Expansion System (ARES) G2 rheometer (TA Instruments, U.S.A.) equipped with an 8 mm parallel plate and a bath trap at a gap of approximately 0.030 mm at 25 °C. The linear response of the PEM was determined by a strain sweep from 0.05% to 100% at frequencies of 0.1 rad/s, 1.0 rad/s, 10.0 rad/s, and 100.0 rad/s. Angular frequency sweeps from 0.1 rad/s to 100.0 rad/s were collected at strain amplitude of 0.50%.

PEM actuation was quantified by the sheet curl degree measurement.²⁸ Each free-standing PEM film was cut into 2 mm × 5 mm pieces, and the specimen was placed on a flat surface and photographed as actuation occurred. To induce actuation of the film, 1.5 μL of the selected solution was dropped onto the BPEI/PAA side of the PEM under ambient conditions. After stabilization of the response to the solvent, a photograph of the specimen was used to calculate the angle of tangent line of the curled end. The mean curl degree was determined by the average value of both sides of the specimen (right and left of image) using 5 measurements for each sample condition.

To test the reversibility of the curling process, the dry flat PEM film was first curled by wetting with 1.5 μL pure ethanol, and the curled film gradually flattened with the evaporation of ethanol and associated sorption of ambient humidity in 15 min. This actuation cycle was repeated 5 times to demonstrate the reversibility of this behavior.

3. RESULTS AND DISCUSSION

The (BPEI_{9.5}/PAA_{4.5})_n film was assembled onto silicon wafers by alternative deposition of BPEI layer and PAA layer based on electrostatics (Scheme 1a).^{25,29} These particular pH values used PE solutions to ensure only partial ionization of BPEI and PAA chains, which results in a thicker deposition with fewer ionic cross-links.²⁵ This particular system is known to grow nonlinearly, and entropic contributions (rather than enthalpic) to film assembly tend to be very large for these types of systems.³⁰ The average dry film thickness of the resultant (BPEI_{9.5}/PAA_{4.5})₆ film is ~264.1 ± 1.2 nm as determined by ellipsometry and ~255 ± 11 nm by profilometer. A slightly lower value given by stylus profilometry is typical as the stylus exerts downward force on the film. The (BPEI_{9.5}/PAA_{4.5})₆ film identically assembled on glass substrate is significantly thicker (~500 nm)²⁹ because of the differences in surface charges of the two substrates.³¹

After being immersed in DI water, the (BPEI_{9.5}/PAA_{4.5})₆ film swells, equilibrating within 5 s, and the thickness increases to 365.8 ± 1.0 nm by ellipsometry. The swelling ratio is calculated as follows:

$$\text{Swelling ratio \%} = \frac{H_s - H_0}{H_0} \times 100 \quad (1)$$

where H_s is the swollen film thickness and H_0 refers to the initial dry thickness of the (BPEI_{9.5}/PAA_{4.5})₆ film.

The swelling ratio of (BPEI_{9.5}/PAA_{4.5})₆ film in pure DI water is ~38.5%, and it progressively decreases as ethanol is added to the solution (Figure 1). With 25 vol % ethanol, the (BPEI_{9.5}/PAA_{4.5})₆ film is still appreciably swollen (~30.0%), but there is actually a contraction in the film thickness (swelling ratio = -6.6%) when the ethanol content is increased to 50 vol % or greater. When soaked in pure ethanol, the film thickness is reduced to 238.7 ± 0.5 nm, which is less than the dry thickness after fabrication (264.1 ± 1.2 nm). In order to ensure that the film is truly contracting and not dissolving, the soaking solution

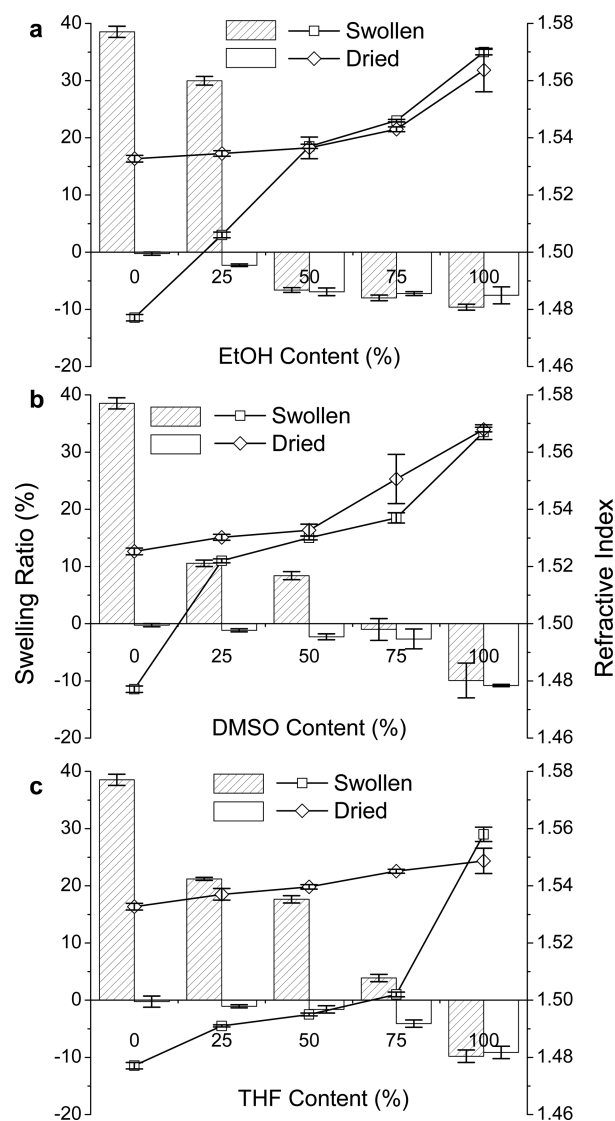


Figure 1. Swelling ratio (bar) and refractive index (line) of the (BPEI_{9.5}/PAA_{4.5})₆ films soaked in different organic solvent/water mixtures and the (BPEI_{9.5}/PAA_{4.5})₆ films dried after this solution treatment. (a) ethanol, (b) DMSO, and (c) THF are respectively applied as the organic solvent.

was drop cast onto silicon wafer and FT-IR spectra was taken (Supporting Information Figure S1). No characteristic absorption bands corresponding to either BPEI or PAA were observed, indicating the reduced film thickness is not caused by dissolution of either PE component into the ethanol–water mixture (or at least not by the loss of enough material to be detectable by FTIR spectroscopy). The nonlinearity of the swelling behavior exhibited by the LbL film in solutions of different composition is likely associated with the large nonideality of the solutions being used. The switch from swelling to contraction occurs between 25 wt % ethanol and 50 wt % ethanol, which corresponds to activities of 0.9 and 0.77 for water (calculated from the van Laar expression). The competition between enthalpy gain from sorption of water and entropy loss from selective partitioning of ethanol into the LbL film is hypothesized to be associated with the change from swelling to contraction with these ethanol–water mixtures. The refractive indices of the (BPEI_{9.5}/PAA_{4.5})₆ films swollen in DI water, 25 vol % ethanol, 50 vol % ethanol, 75 vol % ethanol, and pure ethanol are 1.477,

1.506, 1.537, 1.546, and 1.570. The refractive indices of pure ethanol (1.361) and DI water (1.333)³² are less than that for the dry (BPEI_{9.5}/PAA_{4.5})₆ film (1.531), so sorption of solvent would act to decrease the refractive index of the film. It is noteworthy that the refractive index of the (BPEI_{9.5}/PAA_{4.5})₆ film in ≥ 50 vol % ethanol is even greater than that of the dry film (1.531), which implies these films are densified on exposure to these ethanoic solutions.

After drying overnight in a vacuum oven, the thicknesses of the (BPEI_{9.5}/PAA_{4.5})₆ films exposed to 25 vol % ethanol, 50 vol % ethanol, 75 vol % ethanol, and pure ethanol are still decreased by $\sim 2.3\%$, $\sim 6.9\%$, $\sim 7.2\%$, and $\sim 7.5\%$, respectively (Figure 1a). The refractive indices of these dried films range from 1.535 to 1.560 and are greater than that of the initial dry (BPEI_{9.5}/PAA_{4.5})₆ film (1.531) but slightly lower than that of the film soaked in the corresponding ethanol solutions. This indicates that the film absorbs water from the surrounding environment spontaneously after drying or (less likely) that nanovoids are present in the film that are filled with solvent in the immersed state but the solvent is removed on drying ($n_{\text{air}} \cong 1$). Similarly, deswelling/shrinking behavior is observed for (BPEI_{9.5}/PAA_{4.5})₆ films upon DMSO/water and THF/water exposure (Figure 1b and c), including the decrease in the dried film thickness. The swelling ratio reduces to almost 0% in 75 vol % DMSO aqueous solution, and it drops to -9.9% and -9.8% in pure DMSO and pure THF, respectively. The (BPEI_{9.5}/PAA_{4.5})₆ film tends to deswell or shrink with the more water miscible organic liquid. The organic solvent facilitates the dehydration of PE chains. Thermogravimetric analysis (TGA) data (Supporting Information Figure S2) shows that there is still as much as ~ 7 wt % water in a film dried in a vacuum oven, and the removal of this water corresponds to much of this nearly 10% reduction in film volume. Even once dried after organic solvent exposure, the thickness of the film remains less than the as-prepared dry film thickness. This densification response is in stark contrast to the swelling responses typically reported in LbL assemblies upon exposure to salt³³ or surfactant.³⁴

DLS shows that the average particle size of BPEI is 13.49 nm in water and similar in DMSO and ethanol, only increasing to the micrometer scale in THF, while PAA particle size grows from 12.60 nm in DI water to 255.80 nm in DMSO, 326.35 nm in ethanol, and 435.73 nm in THF (Supporting Information Figure S3). The carboxyl group ionization ratio of the solution treated dry (BPEI_{9.5}/PAA_{4.5})₆ films was calculated from the ratio of the stretching vibration bands of the neutral carboxyl groups (1714 cm^{-1}) and ionized carboxyl groups (1540 cm^{-1}) (Supporting Information Figure S4).^{13,25} Although the ionization ratio slightly decreases to 48.8–52.0% due to the ionization inhibition in low dielectric constant environment,³⁵ the change is slight. PAA is well-known to be extremely hydrophilic, ensuring PAA chain flexibility and possibly enabling superlinear growth of these LbL films. However, exposure to organic solvent creates a gradient in water activity locally within the film and near the film's surface, removing water from the film. This water is not replaced by other solvent nor does the dehydration induce porosity, leading us to believe that the absence of water increases interactions between chain backbones, locally densifying the film.^{36,37} Although these are cross-linked networks, the assembly conditions were chosen to maximize molecular weight between cross-links, meaning that at least locally there is still some mobility and the possibility for the network to rearrange itself, creating a shrunken (BPEI_{9.5}/PAA_{4.5})₆ film that remains so even after drying.

Figure 2a illustrates the reversibility of the swelling/deswelling in water/ethanol through 10 cycles for the (BPEI_{9.5}/PAA_{4.5})₆

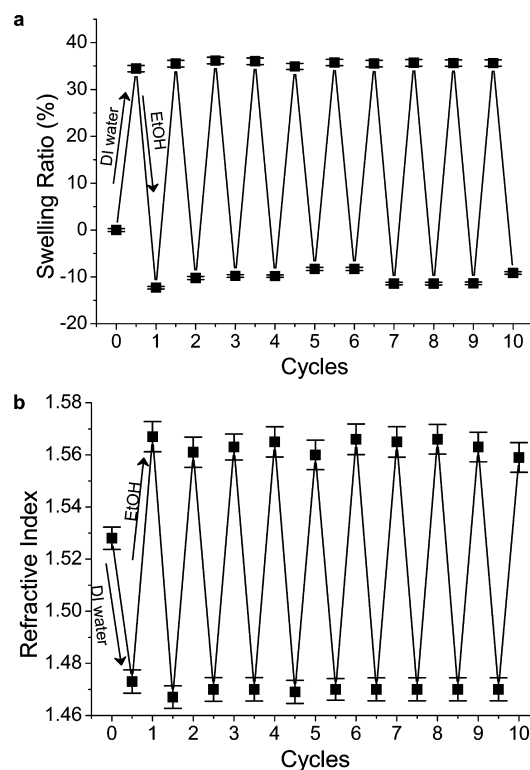


Figure 2. Reversible switching between the swollen and shrunken state of the (BPEI_{9.5}/PAA_{4.5})₆ film in DI water and pure ethanol. (a) Swelling ratio; (b) refractive index.

film as determined by ellipsometry. The film swells $\sim 38.5\%$ in DI water. When immersed in ethanol, the film thickness decreases by ca. 9.6% (Figure 2a). This shrinking response is large when compared to other types of changes seen in PEMs, such as expansion due to heating. For example, hydrogen bonded LbL assemblies are seen to change only $\sim 5\%$ in thickness when being heated over an 80–90 °C temperature range, which includes an apparent T_g .³⁸ Ellipsometry also gives the refractive indices of the film in DI water and ethanol reproducibly as 1.477 and 1.570 (Figure 2), with little variability over repeated cycling. Also, the dried shrunken film repeatedly reswells in DI water within ~ 5 s to the initial hydrated swollen value (Supporting Information Figure S5a). The dry film thickness (after contraction in organic solvent) also returns to the initial state after soaking in water and vacuum drying overnight. At least 10 cycles of swelling/shrinking in water/THF and water/DMSO treatment have been performed on a single film without changes in film performance. The swelling kinetics is significantly faster than the pH and electric field control of PEMs, which requires at least 15 min to induce these changes in the swollen state.³⁹ The maximum swelling ratio in water can be increased by terminating the surface of the film with higher chain mobility polyelectrolyte,⁴⁰ or by changing the pH of the water,¹² while the shrinking response to organic solvent is constant for a given PEM.

For comparison, the response of the strong PE film consisting of (PDAC/SPS)₃₀ in pure ethanol was tested. In pure ethanol, the film thickness of (PDAC/SPS)₃₀ prepared with PE solutions containing no salt remains almost the same as that of the dry state, but the (PDAC/SPS)₃₀ film assembled with 0.1 M NaCl in

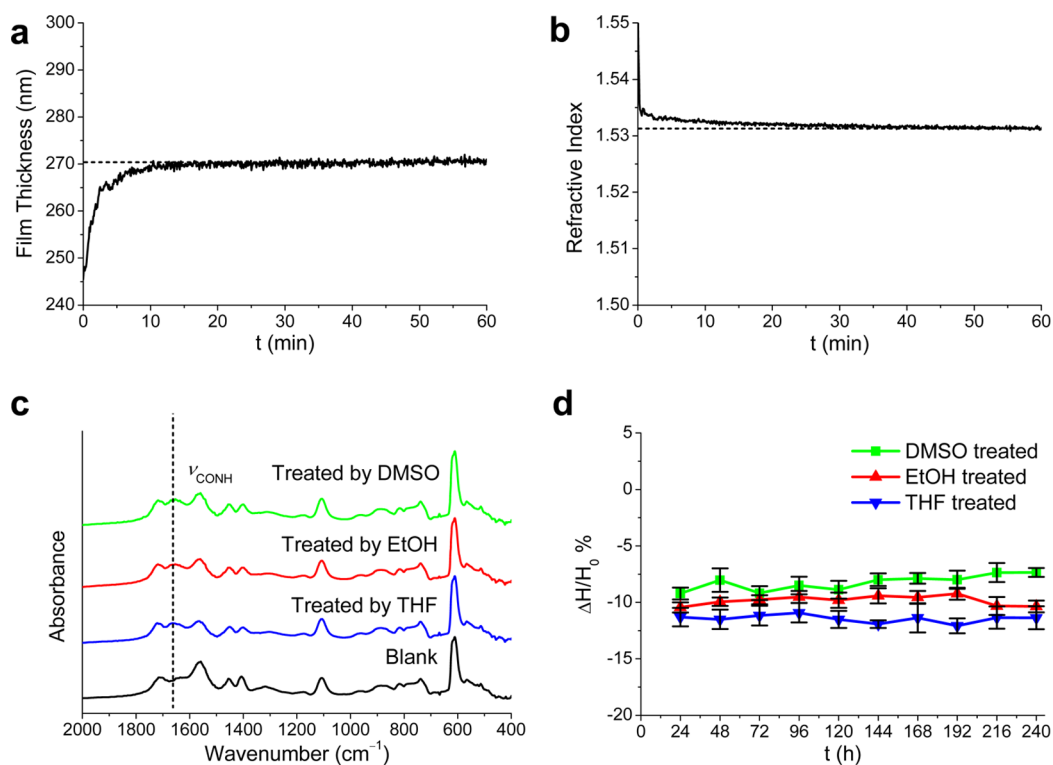


Figure 3. Changes in film thickness (a) and refractive index (b) of (BPEI_{9.5}/PAA_{4.5})₆ film exposed to the ambient conditions (RH ~ 70%, 25 °C) after soaking in THF for 30 min and vacuum drying. (c) FTIR spectra of the as assembled (BPEI_{9.5}/PAA_{4.5})₆ film and the solvent treated (BPEI_{9.5}/PAA_{4.5})₆ film after cross-linking. (d) The change in dry thickness of the cross-linked (BPEI_{9.5}/PAA_{4.5})₆ films compared with the dry as-assembled (BPEI_{9.5}/PAA_{4.5})₆ film; these samples were soaked in different organic solvents prior to the thermal cross-linking treatment.

the PE solutions shrinks ~4.85% compared to the initial dry film. It is known that the presence of added salt compensates the charges along the PE backbones,⁴¹ reducing the ion-pair cross-link density within the PEMs, while the strong polycations and polyanions assembled with no salt in solution are more densely cross-linked with each other in the PEM. The partial neutralization of the strong PEs also results in a solution coil conformation more similar to that of neutral polymers in a good solvent as compared to those solutions with no salt, which then corresponds to the conformation of the PE chains in the film.^{42,43} Without the charge screening from the added salt, electrostatic repulsions result in more extended coil conformations. This in turn corresponds to a greater ionic cross-link density within the multilayer film and a film that is less able to either swell or contract.

Once a THF treated (BPEI_{9.5}/PAA_{4.5})₆ film is dried and then exposed to ambient environment (25 °C, RH ~ 70%), the shrunken film slowly increases in thickness from ~242.1 nm to ~267.4 nm in 20 min (Figure 3a), which agrees with the as assembled film thickness. At the same time, the refractive index decreases from 1.545 to 1.531 over 40 min (Figure 3b), meaning that the (BPEI_{9.5}/PAA_{4.5})₆ film treated with THF gradually returns to its initial state. The hydrophilic PEM film easily absorbs water vapor from the air,⁴⁴ which facilitates hydration of the PE chains and recovery to the film's initial state. Under identical conditions, it takes ~1 h to fully recover the ethanol treated film, and the DMSO treated film thickness remains stable for 24 h, as these solvents are less volatile than THF (and DMSO is relatively nonvolatile). The shrunken state, however, can be fixed by thermal cross-linking. After immersing the film in ethanol, DMSO, or THF for 30 min, the films were heated at 180 °C for 2 h to cross-link the films by formation of amide bonds

from the carboxyl group of PAA and amine groups of BPEI (Figure 3c).²⁵ After cross-linking, the resultant film thickness remains stable for at least 240 h regardless of the organic solvent used to treat the film before thermal cross-linking treatment (Figure 3d).

QCM-D and simultaneous in situ spectroscopic ellipsometry was used to monitor the mass (and thickness) change of the (BPEI_{9.5}/PAA_{4.5})₅ film in ethanol–water mixtures. After equilibrating the film in DI water, the fraction of ethanol in the chamber was increased stepwise until the film was exposed to pure ethanol (10 vol % per step, Supporting Information Figure S5b). Then, the solution was changed back to DI water by stepwise decrease of the ethanol content. The solvent exchange is a relatively slow process due to the residence time of the in situ chamber, partially obfuscating the kinetics of the swelling/deswelling. This is particularly so when the ethanol content is decreased as steady state of both frequency and dissipation take roughly 5 min to be achieved, which is of a similar time scale as the solvent exchange. However, when the ethanol content is increased, the time to reach steady state (stable frequency and dissipation) increases significantly. For example, the change from pure water to 10 vol % ethanol requires nearly 30 min to equilibrate, and this time increases as the ethanol content is increased until 80 min is required to obtain steady state when the 90 vol % ethanol solution is changed to pure ethanol. Both BPEI and PAA are hydrophilic polymers, more easily hydrated than dehydrated, and displacing water for ethanol is a slower process than displacing ethanol for water.⁴⁵

QCM-D was also used to monitor film mass. However, the frequency shift (Δf) and dissipation of the crystal is strongly influenced by the density and viscosity of the liquid overlayer.⁴⁶ The solvent effect on Δf and dissipation, based on analogous

experiments on bare silica crystals (Supporting Information Figure S5c), is subtracted from the data for the $(\text{BPEI}_{9.5}/\text{PAA}_{4.5})_6$ film to enable qualitative interpretation. As shown in Figure 4a,

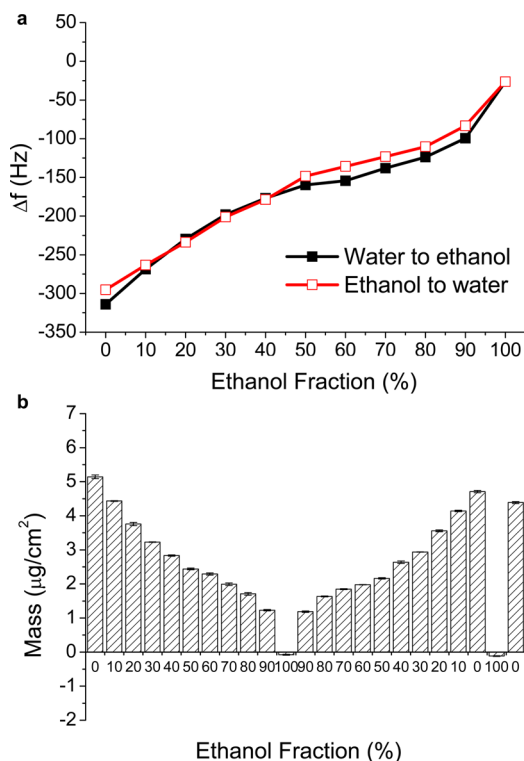


Figure 4. Changes in the apparent equilibrium frequency shift of $(\text{BPEI}_{9.5}/\text{PAA}_{4.5})_6$ film coated silica crystal in comparison to the bare sensor (a) and the liquid mass of the adsorbed solvent in the film at different ethanol fractions (b).

the magnitude of Δf is greatest (-314.0 Hz) in DI water, consistent with water swelling the $(\text{BPEI}_{9.5}/\text{PAA}_{4.5})_6$ to the highest extent for the solutions examined. As the ethanol content is increased, the magnitude of Δf decreases to more than an order of magnitude less for pure ethanol (-26.3 Hz). On reswelling of the film by decreasing the ethanol content, Δf is seen to be reversible, except for a small hysteresis observed in the range 40–100% ethanol. The QCM-D data shows that the swelling behavior is reversible and this is consistent with other measurements indicating that the decrease in the film thickness in pure ethanol is not due to dissolution. Although a similar comprehensive QCM-D study was not performed for the THF and DMSO cases, it has been observed that a film exposed first to 100% solvent and then a 75% solvent solution for these cases is slightly (1–2%) thinner than a film directly exposed to the 75% solvent solution. Thus, it seems that a similar hysteresis in film thickness occurs for all three solvents examined in this work.

To quantify the mass changes, the Sauerbrey expression is applied to the corrected frequencies (Figure 4b). The $(\text{BPEI}_{9.5}/\text{PAA}_{4.5})_6$ film is sufficiently rigid for this analysis as evidenced by the low dissipation ($<10^{-5}$, Supporting Information Figure S5d).⁴⁷ This is consistent with the small deviations from the Sauerbrey expression previously reported for thin PEMs swollen by water (thickness below ~ 400 nm).^{46,48} Initial immersion in water results in significant water sorption leading to an increase in adsorbed liquid mass ($5.1 \mu\text{g}/\text{cm}^2$), but the sorption decreases as the ethanol content is increased, such that the mass of adsorbed liquid in the film decreases to $-0.1 \mu\text{g}/\text{cm}^2$ in pure

ethanol. This decrease in mass is consistent with a dehydration accompanying the film shrinkage. It should be noted that the mass measured by QCM-D when immersed in a fluid is the coupled mass, which can include bound or hydrodynamically coupled solvent. This behavior tends to overpredict the sorbed mass in QCM-D.⁴⁷ Thus, the reported mass loss on immersion in ethanol is the lower limit, and the loss could be slightly greater.

In addition, as the corrected frequency change is relative to the blank crystal, the original dry film mass is known to be $27.34 \pm 0.02 \mu\text{g}/\text{cm}^2$ for a 287.6 ± 1.6 nm thick $(\text{BPEI}_{9.5}/\text{PAA}_{4.5})_6$ film. Thus, the density of the as prepared dry film is $1.05 \text{ g}/\text{cm}^3$. The total mass of the film is $27.27 \pm 0.02 \mu\text{g}/\text{cm}^2$ in pure ethanol from the Sauerbrey expression. The film thickness in ethanol decreases to 238.7 nm, which gives a film density of $1.14 \text{ g}/\text{cm}^3$. This unexpected nearly 10% increase in density of the $(\text{BPEI}_{9.5}/\text{PAA}_{4.5})_6$ film on immersion in ethanol is consistent with film shrinkage without dissolution and is large in magnitude. This film can be reversibly swollen/deswollen by switching from DI water to pure ethanol results in nearly identical mass changes as observed for the gradual stepwise changes (Figure 4b). The water mass taken up by the film slightly decreases when the solution is changed from pure ethanol to DI water directly, because the equilibration time (30 min) is much shorter than the stepwise solution change from pure ethanol to DI water (>200 min).

Although the QCM-D dissipation shift suggests a decrease of film viscosity in higher ethanol fraction solution (Supporting Information Figure S5d), the dissipation shift is too small for accurate modeling by Voigt model to extract the related shear modulus and viscosity.⁴⁹ Therefore, the shear storage and loss moduli of the BPEI/PAA multilayer film soaked in these solutions were measured by rheometry. To maintain the swollen state of the film during the course of the experiment, a plate fixture with a solvent trap was used. A free-standing $(\text{BPEI}_{9.5}/\text{PAA}_{4.5})_{50}$ film was soaked in the selected solution for 5 min to equilibrate prior to testing, and an axial force >20 N was applied to exclude the possible liquid influence. After immersing the initially elastic dry $(\text{BPEI}_{9.5}/\text{PAA}_{4.5})_{50}$ film in DI water, both the storage modulus G' and loss modulus G'' of the film increase exponentially with applied angular frequency (Figure 5a). In this case, $G''(\omega) > G'(\omega)$, indicating a liquid-like behavior of the film in DI water.⁵⁰ With the addition of ethanol in the solution, a stepwise increase in both G' and G'' of the film are observed (Supporting Information Figure S11). Once soaked in pure ethanol, $G'(\omega)$ dominates, and $G'(\omega)$ and $G''(\omega)$ become nearly invariant to frequency change (Figure 5a and Supporting Information Figure S10d), which is indicative of a viscoelastic solid. The relaxation time of BPEI/PAA in pure ethanol estimated from the extended moduli curve cross-point is 2.9×10^7 s. This is far longer than the $(\text{BPEI}_{9.5}/\text{PAA}_{4.5})_{50}$ film in DI water (~ 0.01 s). Even the recently reported poly(*N,N*-dimethylaminoethyl methacrylate)/PAA complex coacervates with dense ionically bonded sticky points (~ 1000 s) exhibit orders of magnitude faster relaxation times.⁵⁰ This extremely long relaxation time supports the notion that there are increased secondary interactions. In ethanol, G' reaches a plateau of ~ 2.68 MPa. This exceeds the storage moduli of the dry $(\text{BPEI}_{9.5}/\text{PAA}_{4.5})_{50}$ film ($G' \sim 129$ kPa, Supporting Information Figure S12) and water soaked film as well by more than an order of magnitude. Compared to other LbL systems, this modulus is higher than poly(allylamine hydrochloride)/SPS multilayer film swollen in water (~ 230 kPa) and after further deswelling by applying electric field (~ 1.90 MPa).¹² Meanwhile, G'' of the $(\text{BPEI}_{9.5}/\text{PAA}_{4.5})_{50}$ film in pure ethanol (65.0 kPa) is far lower

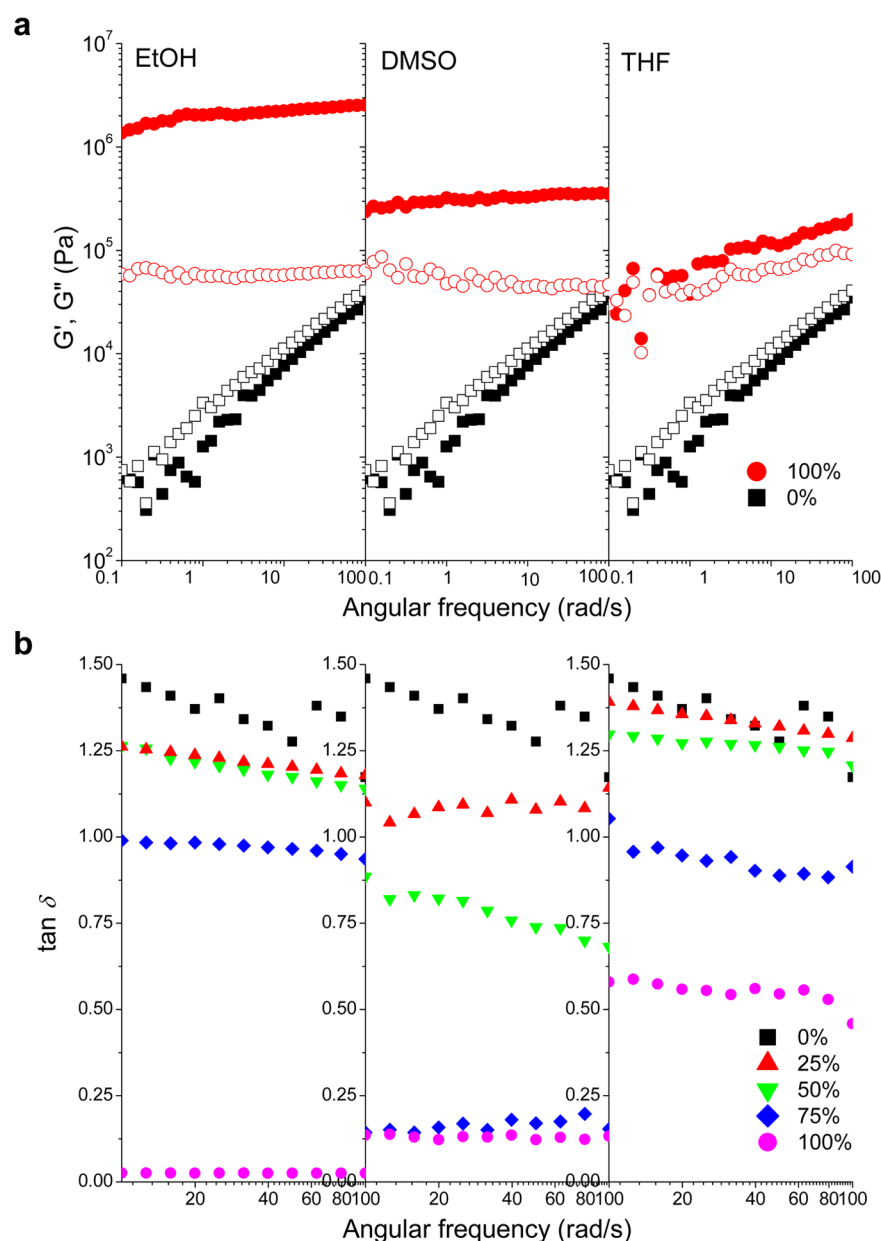


Figure 5. (a) Angular frequency sweep plot by 0.5% strain at 25 °C for (BPEI_{9.5}/PAA_{4.5})₅₀ film soaked in DI water (0%) or pure organic solvents (100%) for G' (closed symbols) and G'' (open symbols). (b) Loss factor, $\tan \delta$, by angular frequency sweep for (BPEI_{9.5}/PAA_{4.5})₅₀ film in organic solvent/water solutions.

than that the stimuli-responsive poly(allylamine hydrochloride)/SPS multilayer film (~92 kPa in water and ~620 kPa deswollen by external electric field).¹² These results demonstrate that the film acts as a cross-linked solid in ethanol.

As shown in Figure 5b, by increasing ethanol content in the solution, the loss factor, $\tan \delta$ (G''/G'), reduces from ~1.50 to nearly 0, indicating a gradual transition from a viscous liquid to an elastic solid.⁵⁰ From DI water to 75 vol % ethanol, the loss factor slowly reduces, and it drops drastically to 0.025 in pure ethanol, agreeing with the shrinkage of BPEI/PAA multilayers. When soaked in DMSO and THF, similar transformation from viscous to elastic is observed for the (BPEI_{9.5}/PAA_{4.5})₅₀ film (Figure 5, Supporting Information Figures S16 and S21). In both cases, G' (ω) dominate within the angular frequency from 0.1 to 100.0 rad/s. The respective relaxation times for the film in DMSO and THF are estimated as 2116 and 39.8 s, both of which are much

longer than in DI water. While G'' remains almost unchanged, G' and the relaxation time decrease from ethanol, DMSO, to THF.

The DI water soaked film is very sticky and highly stretchable, but the film soaked in organic solvent is brittle (Supporting Information Figure S23). This is demonstrated by Supporting Information Video S1 in which films are stretched (1) under ambient conditions, (2) wet with DI water, and (3) wet with DMSO. One can see that the film under the ambient humidity is slightly stretchable, the film wet with water acts as a viscoelastic material and does not break, whereas the film wet with DMSO is brittle and fractures almost immediately upon application of strain. Supporting Information Video S2 shows that a film immersed in water is soft and breaks when a small metal ball bearing is placed on its surface, whereas the same film immersed in ethanol can support the weight of the ball bearing. Although exposure to all organic solvents increases the strength of the LbL

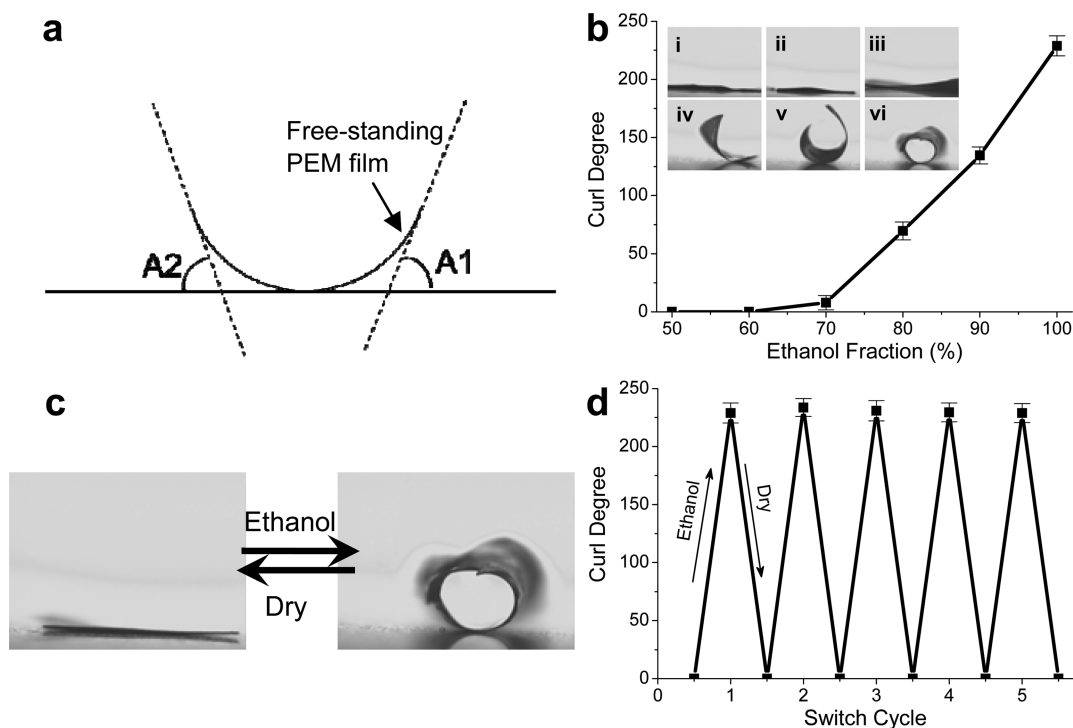


Figure 6. (a) Schematic illustration of the determination of the curl degree, which is defined as the average of angles A1 and A2. (b) Curl degrees of the free-standing (BPEI_{9.5}/PAA_{4.5})₅₀/(PDAC/SPS)₅₀ film treated by solutions with different ethanol content. The insets show the photographs of the film treated by 50 vol % (i), 60 vol % (ii), 70 vol % (iii), 80 vol % (iv), 90 vol % (v), and 100 vol % ethanol (vi). Photographs (c) and curl degree (d) of the (BPEI_{9.5}/PAA_{4.5})₅₀/(PDAC/SPS)₅₀ film in dry state and wetted by ethanol.

films, exposure to the most water miscible/most hydrophilic solvent results in the stiffest film. The higher water miscibility may facilitate complete solvent exchange, which, in turn, will more completely change the dielectric environment around the ion bond pairs.

Exposure to organic solvent results in an extensive prolongation in the relaxation time by several orders of magnitude and an increase in rigidity occurs along with film shrinkage and densification. These changes are the result of a dehydration of the PE components in the film, reducing the film volume. Increasing refractive index and density show that the dehydration is accompanied by a densification, meaning that individual polymer chains are closer to one another after the hydration shell is removed. The charge density of the PAA chains remains similar in organic solvent as in water, but the dielectric constant (ϵ) of the surrounding environment has significantly decreased. One can estimate the force of the ionic bonding by Coulomb's law:⁵¹

$$F = \frac{Q_1 Q_2}{4\pi\epsilon_0\epsilon r^2} \quad (2)$$

The reduction in ϵ in organic solvent significantly increases the Coulombic force between ion pairs in the PEM. When compared with the film in DI water ($\epsilon = 78.48$),⁵² the Coulombic force is 3.2, 1.7, and 10.6 times higher in ethanol ($\epsilon = 24.55$), DMSO ($\epsilon = 46.7$), and THF ($\epsilon = 7.39$), respectively. For partially ionized BPEI and PAA, the ionic cross-link density is lower than for films made from fully charged chains and the film can swell in water. However, the exposure to organic solvent densifies the (BPEI_{9.5}/PAA_{4.5})₆ film, enhancing the effective friction between chains and reducing chain mobility.⁵⁰ The film is stiffer in this reduced mobility environment in which the ion pairs are more difficult to

pull apart. Although the dielectric constant of THF is lowest of the solvents examined, immersion in ethanol results in the strongest film. One possible explanation is that ethanol is the most hydrophilic of these solvents, perhaps enabling more complete exchange of solvent (i.e., extraction of water from the PEM). In the case of immersion in THF, a solvation shell of water may remain near the charged ionic groups, mitigating the effect of the lower dielectric constant medium.

The results reported here contrast with reports showing that poly(allylamine hydrochloride)/SPS capsules becoming softer in response to exposure to water/ethanol or water/acetone mixtures. The current results indicate that both an increase in interchain hydrophobic interactions caused by a loss of the hydration shell around the PE chains and strengthening of the ion-pair bonds due to changes in dielectric constant contribute to the stiffening and densification of the PEM. In this case, perhaps swelling is achieved from the difference in chemical potential between the pure water (neutral polymer for some of these reports) in the core of the capsules and the solvent/water mixture presented to the outside of the capsules and this osmotic pressure may overwhelm the other changes that occur due to the exposure to the organic solvent.

By taking advantage of the distinct swelling/shrinking behaviors of different types of PEM material upon organic liquid treatment, a PEM film with large scale actuation was prepared via successive LbL assembly of 50 BPEI/PAA bilayers and 50 PDAC/SPS bilayers. The finished free-standing film has an asymmetrical structure in the direction of film growth. One side consists of an organic solvent-responsive BPEI/PAA layer and the other side of a PDAC/SPS layer that does not exhibit the same response. This asymmetric structure enables selective curl toward the BPEI/PAA side upon ethanol treatment, which is not possible for a (BPEI_{9.5}/PAA_{4.5})₅₀ only film similarly exposed to

ethanol. The actuation was characterized by calculating a “curl degree” defined as

$$\text{Curl degree} = \frac{A1 + A2}{2} \quad (3)$$

where A1 and A2 are the curled angle of left end and right end of the sample edges, respectively (Figure 6a).²⁸ The as-prepared free-standing (BPEI_{9.5}/PAA_{4.5})₅₀/(PDAC/SPS)₅₀ film bends within 2 s when 70 vol % ethanol is applied, and the average film curl degree increases to ~7.8°, ~69.6°, ~134.6°, and ~228.9° with 70 vol %, 80 vol %, 90 vol %, and pure ethanol exposure (Figure 6b). In short, the higher the ethanol content, the more the film curls, as the BPEI/PAA contracts while the PDAC/SPS does not. This system either curls more significantly than other examples of self-assembled PE systems⁵⁵ or more quickly.⁵⁴ Moreover, the curled free-standing (BPEI/PAA)₅₀/(PDAC/SPS)₅₀ film gradually return to the initial flat state (curl degree ~0°, Figure 6c) with the evaporation of the ethanol under ambient conditions as the ethanol is exchanged for water. Figure 6d shows that the film can be reversible cycled between curled and flat states at least 5 times.

4. CONCLUSIONS

A unique and fully recoverable shrinking and densification of BPEI/PAA PEMs in organic/aqueous solutions was demonstrated, accompanied by a transition in rheological properties from a viscous fluid to a rigid solid. In the presence of water miscible organic solvents, the strength of the ionic cross-links within the multilayer is increased and hydrophobic interactions are increased as well, causing this change of properties. BPEI/PAA PEMs contract up to 9.6% in thickness in pure organic solvent. Ellipsometry and QCM-D demonstrate that swelling in water as well as contraction in organic solvent is repeatable and fully recoverable between 38.5% swelling in water and a 9.6% contraction in pure ethanol. Under ambient conditions, the film will recover its initial thickness due to spontaneous rehydration in the ambient humidity. Covalent cross-links formed thermally between the amine and carboxylic acid groups can, however, fix the contracted film thickness permanently. Increased density in a thin polymer film may be advantageous for separation membranes or barrier properties. This controllable swelling behavior is accompanied by the rheological transition of the film from viscous to elastic. The strong PE system PDAC/SPS does not have the same type of behavior, and we have demonstrated large scale solvent driven actuation of a (BPEI/PAA)/(PDAC/SPS) bilayer film. Considering that fabrication of PEMs has been realized using industrial-scale techniques,⁵⁵ this smart PEM film actuator can be applied as actuators, sensors, motors, and automated gates for industry and daily life. The current work sheds light on the use of dynamic secondary interactions to create large-scale mechanical response in weak PEMs, which may be used as a new pathway to create mechanical motion in PEMs from a chemical stimulus.

■ ASSOCIATED CONTENT

Supporting Information

The FT-IR spectra of the bare (BPEI_{9.5}/PAA_{4.5})₆ film and film soaked solutions; TGA plot of the bare (BPEI_{9.5}/PAA_{4.5})₆ film; ionization ratio of solution soaked films after drying; photographs of the stretched films; strain sweep and angular frequency sweep plots of the (BPEI_{9.5}/PAA_{4.5})₆ film soaked in various solutions and dry film. This material is available free of charge via the Internet at <http://pubs.acs.org>.

■ AUTHOR INFORMATION

Corresponding Author

*E-mail: nzacharia@uakron.edu.

Notes

The authors declare no competing financial interest.

■ ACKNOWLEDGMENTS

This work was supported by National Science Foundation (NSF) grant 1425187 and the Department of Polymer Engineering at the University of Akron.

■ REFERENCES

- (1) Ariga, K.; Hill, J. P.; Ji, Q. Layer-by-Layer Assembly as a Versatile Bottom-up Nanofabrication Technique for Exploratory Research and Realistic Application. *Phys. Chem. Chem. Phys.* **2007**, *9*, 2319–2340.
- (2) Sukhishvili, S. A. Responsive Polymer Films and Capsules via Layer-by-Layer Assembly. *Curr. Opin. Colloid Interface Sci.* **2005**, *10*, 37–44.
- (3) Quinn, J. F.; Pas, S. J.; Quinn, A.; Yap, H. P.; Suzuki, R.; Tuomisto, F.; Shekibi, B. S.; Mardel, J. I.; Hill, A. J.; Caruso, F. Tailoring the Chain Packing in Ultrathin Polyelectrolyte Films Formed by Sequential Adsorption: Nanoscale Probing by Positron Annihilation Spectroscopy. *J. Am. Chem. Soc.* **2012**, *134*, 19808–19818.
- (4) Bucur, C. B.; Sui, Z.; Schlenoff, J. B. Ideal Mixing in Polyelectrolyte Complexes and Multilayers: Entropy Driven Assembly. *J. Am. Chem. Soc.* **2006**, *128*, 13690–13691.
- (5) Priftis, D.; Laugel, N.; Tirrell, M. Thermodynamic Characterization of Polypeptide Complex Coacervation. *Langmuir* **2012**, *28*, 15947–15957.
- (6) Nguyen, P. M.; Zacharia, N. S.; Verploegen, E.; Hammond, P. T. Extended Release Antibacterial Layer-by-Layer Films Incorporating Linear-Dendritic Block Copolymer Micelles. *Chem. Mater.* **2007**, *19*, 5524–5530.
- (7) Gu, Y.; Liu, X.; Niu, T.; Huang, J. Superparamagnetic Hierarchical Material Fabricated by Protein Molecule Assembly on Natural Cellulose Nanofibres. *Chem. Commun.* **2010**, *46*, 6096–6098.
- (8) Gu, Y.; Huang, J. Ultrathin Cellulose Film Coating of Porous Alumina Membrane for Adsorption of Superoxide Dismutase. *J. Mater. Chem. B* **2013**, *1*, 5636–5643.
- (9) Gu, Y.; Niu, T.; Huang, J. Functional Polymeric Hybrid Nanotubular Materials Derived from Natural Cellulose Substances. *J. Mater. Chem.* **2010**, *20*, 10217–10223.
- (10) Gu, Y.; Huang, J. Fabrication of Natural Cellulose Substance derived Hierarchical Polymeric Materials. *J. Mater. Chem.* **2009**, *19*, 3764–3770.
- (11) Weatherspoon, M. R.; Cai, Y.; Crne, M.; Srinivasarao, M.; Sandhage, K. H. 3D Rutile Titania-Based Structures with Morpho Butterfly Wing Scale Morphologies. *Angew. Chem., Int. Ed.* **2008**, *47*, 7921–7923.
- (12) Schmidt, D. J.; Min, Y.; Hammond, P. T. Mechanomutable and Reversibly Swellable Polyelectrolyte Multilayer Thin Films Controlled by Electrochemically induced pH Gradients. *Soft Matter* **2011**, *7*, 6637–6647.
- (13) Choi, J.; Rubner, M. F. Influence of the Degree of Ionization on Weak Polyelectrolyte Multilayer Assembly. *Macromolecules* **2005**, *38*, 116–124.
- (14) Li, Y.; Chen, S.; Wu, M.; Sun, J. Polyelectrolyte Multilayers Impart Healability to Highly Electrically Conductive Films. *Adv. Mater.* **2012**, *24*, 4578–4582.
- (15) Lindhoud, S.; Stuart, M. A. C. Relaxation Phenomena during Polyelectrolyte Complex Formation. *Adv. Polym. Sci.* **2014**, *255*, 139–172.
- (16) Essafi, W.; Abdelli, A.; Bouajila, G.; Boué, F. Behavior of Hydrophobic Polyelectrolyte Solution in Mixed Aqueous/Organic Solvents Revealed by Neutron Scattering and Viscosimetry. *J. Phys. Chem. B* **2012**, *116*, 13525–13537.

- (17) Kim, B.-S.; Lebedeva, O. V.; Koynov, K.; Gong, H.; Glasser, G.; Lieberwith, I.; Vinogradova, O. I. Effect of Organic Solvent on the Permeability and Stiffness of Polyelectrolyte Multilayer Microcapsules. *Macromolecules* **2005**, *38*, 5214–5222.
- (18) Huang, H. C.; Zacharia, N. S. Polyelectrolyte Multilayers and Complexes to Modify Secondary Interactions in Ethylene comethacrylic Acid Ionomers. *ACS Macro Lett.* **2012**, *1*, 209–212.
- (19) Tettey, K. E.; Yee, M. Q.; Lee, D. Layer-by-Layer Assembly of Charged Particles in Nonpolar Media. *Langmuir* **2010**, *26*, 9974–9980.
- (20) Kim, B.-S.; Lebedeva, O. V.; Park, M. K.; Knoll, W.; Caminade, A. M.; Majoral, J. P.; Vinogradova, O. I. THF-Induced Stiffening of Polyelectrolyte/Phosphorus Dendrimer Multilayer Microcapsules. *Polymer* **2010**, *51*, 4525–4529.
- (21) Kim, B.-S.; Lebedeva, O. V.; Koynov, K.; Gong, H.; Glasser, G.; Lieberwith, I.; Vinogradova, O. I. Effect of Organic Solvent on the Permeability and Stiffness of Polyelectrolyte Multilayer Capsules. *Macromolecules* **2005**, *38*, 5214–5222.
- (22) Lvov, Y.; Antipov, A. A.; Mamedov, A.; Moehwald, H.; Sukhorukov, G. B. Urease Encapsulation in Nanoorganized Microshells. *Nano Lett.* **2001**, *1*, 125–128.
- (23) Lulevich, V. V.; Radtchenko, I. L.; Sukhorukov, G. B.; Vinogradova, O. I. Mechanical Properties of Polyelectrolyte Microcapsules Filled with a Neutral Polymer. *Macromolecules* **2003**, *36*, 2832–2837.
- (24) Joseph, N.; Ahmadiannamini, P.; Hoogenboom, R.; Vankelecom, I. F. J. Layer-by-Layer Preparation of Polyelectrolyte Multilayer Membranes for Separation. *Polym. Chem.* **2014**, *5*, 1817–1831.
- (25) Huang, X.; Chrisman, J. D.; Zacharia, N. S. Omniphobic Slippery Coatings Based on Lubricant-Infused Porous Polyelectrolyte Multilayers. *ACS Macro Lett.* **2013**, *2*, 826–829.
- (26) Qiang, Z.; Xue, J.; Cavicchi, K. A.; Vogt, B. D. Morphology Control in Mesoporous Carbon Films using Solvent Vapor Annealing. *Langmuir* **2013**, *29*, 3428–3438.
- (27) Herzinger, C.; Johs, B.; McGahan, W. A.; Woollam, J. A.; Paulson, W. Ellipsometric Determination of Optical Constants for Silicon and Thermallygrown Silicon Dioxide via a Multi-Sample, Multi-Wavelength, Multi-Angle Investigation. *J. Appl. Phys.* **1998**, *83*, 3323–3336.
- (28) Carson, F. T.; Worthington, V. Measuring the Degree of Curl of Paper. *J. Res. Natl. Bur. Stand. (U.S.)* **1943**, *30*, 113–121.
- (29) Huang, X.; Bolen, M. J.; Zacharia, N. S. Silver Nanoparticle Aided Self-Healing of Polyelectrolyte Multilayers. *Phys. Chem. Chem. Phys.* **2014**, *16*, 10267–10273.
- (30) Laugel, N.; Betscha, C.; Winterhalter, M.; Voegel, J. C.; Schaaf, P.; Ball, V. Relationship between the Growth Regime of Polyelectrolyte Multilayers and the Polyanion/Polycation Complexation Enthalpy. *J. Phys. Chem. B* **2006**, *110*, 19443–19449.
- (31) Hau, W. L. W.; Trau, D. W.; Sucher, N. J.; Wong, M.; Zohar, Y. Surface-Chemistry Technology for Microfluidics. *J. Micromech. Microeng.* **2003**, *13*, 272–278.
- (32) Scott, T. A., Jr. Refractive Index of Ethanol–Water Mixtures and Density and Refractive Index of Ethanol–Water–Ethylether Mixtures. *J. Phys. Chem.* **1946**, *50*, 406–412.
- (33) Dubas, S. T.; Schlenoff, J. B. Swelling and Smoothing of Polyelectrolyte Multilayers by Salt. *Langmuir* **2001**, *17*, 7725–7727.
- (34) Kang, J.; Dähne, L. Strong Response of Multilayer Polyelectrolyte Films to Cationic Surfactants. *Langmuir* **2011**, *27*, 4627–4634.
- (35) Sarmini, K.; Kennidler, E. Ionization Constants of Weak Acids and Bases in Organic Solvents. *J. Biochem. Biophys. Methods* **1999**, *38*, 123–137.
- (36) Moniruzzaman, M.; Sabey, C. J.; Fernando, G. F. Photoresponsive Polymers: An Investigation of Their Photoinduced Temperature Changes during Photoviscosity Measurements. *Polymer* **2007**, *48*, 255–263.
- (37) Branham, K. D.; Shafer, G. S.; Hoyle, C. E.; McCormick, C. L. Water-Soluble Copolymers. 61. Microstructural Investigation of Pyrenesulfonamide-Labeled Polyelectrolytes. Variation of Label Proximity utilizing Micellar Polymerization. *Macromolecules* **1995**, *28*, 6175–6182.
- (38) Sung, C.; Vidyasagar, A.; Hearn, K.; Lutkenhaus, J. L. Effect of Thickness on the Thermal Properties of Hydrogen-Bonded LbL Assemblies. *Langmuir* **2012**, *28*, 8100–8109.
- (39) Lee, D.; Nolte, A. J.; Kunz, A. L.; Rubner, M. F.; Cohen, R. E. pH-Induced Hysteretic Gating of Track-Etched Polycarbonate Membranes: Swelling/Deswelling Behavior of Polyelectrolyte Multilayers in Confined Geometry. *J. Am. Chem. Soc.* **2006**, *128*, 8521–8529.
- (40) Miller, M. D.; Bruening, M. L. Correlation of the Swelling and Permeability of Polyelectrolyte Multilayer Films. *Chem. Mater.* **2005**, *17*, 5375–5381.
- (41) Heuvingh, J.; Zappa, M.; Fery, A. Salt Softening of Polyelectrolyte Multilayer Capsules. *Langmuir* **2005**, *21*, 3165–3171.
- (42) Klitzing, R. V. Internal Structure of Polyelectrolyte Multilayer Assemblies. *Phys. Chem. Chem. Phys.* **2006**, *8*, 5012–5033.
- (43) Schoenhoff, M. Layered Polyelectrolyte Complexes: Physics of Formation and Molecular Properties. *J. Phys.: Condens. Matter* **2003**, *15*, R1781.
- (44) Wong, J. E.; Rehfeldt, F.; Hänni, P.; Tanaka, M.; Klitzing, R. v. Swelling Behavior of Polyelectrolyte Multilayers in Saturated Water Vapor. *Macromolecules* **2004**, *37*, 7285–7289.
- (45) Terech, P.; Weiss, R. G. Low Molecular Mass Gelators of Organic Liquids and the Properties of Their Gels. *Chem. Rev.* **1997**, *97*, 3133–3160.
- (46) Kanazawa, K. K.; Gordon, J. G., II. Frequency of a Quartz Microbalance in Contact with Liquid. *Anal. Chem.* **1985**, *57*, 1770–1771.
- (47) Vogt, B. D.; Lin, E. K.; Wu, W.-L.; White, C. C. Effect of Film Thickness on the Validity of the Sauerbrey Equation for Hydrated Polyelectrolyte Films. *J. Phys. Chem. B* **2004**, *108*, 12685–12690.
- (48) Wiener, C. G.; Weiss, R. A.; Vogt, B. D. Overcoming Confinement Limited Swelling in Hydrogel Thin Films using Supramolecular Interactions. *Soft Matter* **2014**, *10*, 6705–6712.
- (49) Craig, V. S. J.; Plunkett, M. Determination of Coupled Solvent Mass in Quartz Crystal Microbalance Measurements using Deuterated Solvents. *J. Colloid Interface Sci.* **2003**, *262*, 126–129.
- (50) Spruijt, E.; Stuart, M. A. C.; van der Gucht, J. Linear Viscoelasticity of Polyelectrolyte Complex Coacervates. *Macromolecules* **2013**, *46*, 1633–1641.
- (51) Hiemenz, P. C.; Rajagopalan, R. *Principles of Colloid and Surface Chemistry*, 3rd ed; CRC Press: New York, 1997.
- (52) Critchfield, F. E.; Gibson, J. A., Jr.; Hall, J. L. Dielectric Constant and Refractive Index from 20 to 35° and Density at 25° for the System Tetrahydrofuran–Water. *J. Am. Chem. Soc.* **1953**, *75*, 6044–6045.
- (53) Zhao, Q.; Dunlop, J. W.; Qiu, X.; Huang, F.; Zhang, Z.; Heyda, J.; Dzubiel, J.; Antonietti, M.; Yuan, J. An Instant Multi-Responsive Porous Polymer Actuator Driven by Solvent Molecule Sorption. *Nat. Commun.* **2014**, *5*, 4293.
- (54) Shen, L.; Fu, J.; Picart, C.; Ji, J. Humidity Responsive Asymmetric Free-Standing Multilayer Films. *Langmuir* **2010**, *26*, 16634–16637.
- (55) Krogman, K. C.; Cohen, R. E.; Hammond, P. T.; Rubner, M. F.; Wang, B. N. Industrial-Scale Spray Layer-by-Layer Assembly for Production of Biomimetic Photonic Systems. *Bioinspiration Biomimetics* **2013**, *8*, 045005.